CHIN. PHYS. LETT. Vol. 33, No. 1 (2016) 016102

Effect of Al Addition on the Glass-Forming Ability and Magnetic Properties of a Gd–Co Binary Amorphous Alloy *

Cheng Wu(武城), Ding Ding(丁鼎)**, Lei Xia(夏雷)

Laboratory for Microstructure, Institute of Materials, Shanghai University, Shanghai 200072

(Received 28 September 2015)

The glass-forming ability (GFA) and magnetic properties of the $Gd_{50}Co_{50}$-based amorphous alloy with Al addition substitution for Co are investigated. It is found that the GFA and magneto-caloric effect of the $Gd_{50}Co_{45}Al_5$ amorphous alloy are better than $Gd_{50}Co_{50}$ amorphous alloy. The maximum magnetic entropy change ($-\Delta S_{\rm m}^{\rm peak}$) and the magnetic refrigerant capacity of the amorphous alloy under a field of 5 T are about 6.64 $J{\cdot}kg^{-1}K^{-1}$ and 764 $J{\cdot}kg^{-1}$, respectively. The field dependence of magnetic entropy change meets the one predicted by the mean field theory, which is investigated for a better understanding of the magneto-caloric behaviors of the $Gd_{50}Co_{45}Al_5$ amorphous alloy.

PACS: 61.43.Dq, 81.05.Kf, 75.30.Sg, 81.20.−n DOI: 10.1088/0256-307X/33/1/016102

For decades, magnetic refrigeration (MR) has attracted tremendous attention due to the fact that it is regarded as an environmentally friendly and highly efficient technology.[1,2] In contrast to traditional vapor-compression refrigeration, the MR was slowing the destruction of the ozone layer, reducing emissions of greenhouse gases and saving as much as 30% energy cost. MR is based on the magneto-caloric effect (MCE), which refers to the adiabatic temperature change of the magnetic materials with the variation of an applied magnetic field. In a magnetic refrigeration system, the better working substances with excellent MCE are essential.

Amorphous alloys, exhibiting unique properties[3–6] such as good mechanical properties and corrosion resistance, low energy loss large electric resistance and nearly zero magnetic hysteresis, are suitable to be the working substances in magnetic refrigeration systems. Numerous amorphous alloys with excellent MCE have been developed in recent decades.[7–16] Most amorphous alloys undergo second-order magnetic phase transition, and usually show broadened $\Delta S_{\rm m}$ peaks. The broadened $\Delta S_{\rm m}$ peaks lead to the high refrigerant capacity (RC) but a lower $\Delta S_{\rm m}^{\rm peak}$. Therefore, one of the most important topics for the use of amorphous magnetic refrigerants is how to improve their $\Delta S_{\rm m}^{\rm peak}$.

Alloying addition has already shown dramatic effects on GFA and magnetic properties of the amorphous alloys.[17,18] To investigate the influence of Al substitution for Co on GFA, Curie temperature ($T_{\rm C}$) and MCE of $Gd_{50}Co_{50}$-based amorphous alloy, in this Letter we study the GFA and magnetic properties of the $Gd_{50}Co_{45}Al_5$ alloy, compared with the $Gd_{50}Co_{50}$ alloy. It is found that the GFA and MCE of the $Gd_{50}Co_{45}Al_5$ amorphous alloys are better than the $Gd_{50}Co_{50}$ amorphous alloy. The field dependence of magnetic entropy change is investigated for a better understanding on the magneto-caloric behaviors of the $Gd_{50}Co_{45}Al_5$ amorphous alloy.

A $Gd_{50}Co_{45}Al_5$ ingot was prepared by arc-melting a mixture of Gd, Co and Al elements with a purity of above 99.9% (at%). The ingot was re-melted for at least four times to ensure the homogeneity of the ingot under a Ti-gettered argon atmosphere, and then re-melted and spun to produce a ribbon by a single-roller in a high-purified argon atmosphere. The amorphous characteristic of the $Gd_{50}Co_{45}Al_5$ as-spun ribbon was confirmed by x-ray diffraction (XRD) on a Rigaku D\max-2550 diffractometer by using Cu K_α radiation. The glass transition temperature $T_{\rm g}$ and the crystallization temperature T_x were obtained by a Perkin–Elmer DIAMOND differential scanning calorimetry (DSC) at a heating rate of 20 K/min under a purified nitrogen atmosphere, while the liquidus temperature $T_{\rm l}$ and the melting temperature $T_{\rm m}$ were measured by a NETZSCH 404C high temperature DSC at the same heating rate. The magnetic properties of the amorphous ribbon were measured by a quantum design physical property measurement system (PPMS): the temperature dependence of magnetization (M–T) curves was measured under the field of 0.03 T during the cooling process and the isothermal magnetization curves (M–H) were performed at a selected temperature under a field of 5 T.

The XRD pattern and DSC traces, as shown in Fig. 1, illustrate a typical amorphous characteristic of the $Gd_{50}Co_{45}Al_5$ as-spun ribbon. Here $T_{\rm g}$ = 547 K and T_x = 588 K of the ribbon are obtained from the DSC trace at a heating rate of 20 K/min, as marked

*Supported by the National Natural Science Foundation of China under Grant Nos 51171100 and 51271103, and the Research Grants Council of the Hong Kong Special Administrative Region under Grant No PolyU511212.

**Corresponding author. Email: d.ding@shu.edu.cn

© 2016 Chinese Physical Society and IOP Publishing Ltd

clearly in Fig. 1(b). The melting behavior of the ribbon is shown in the inset of Fig. 1(b). The values of T_m and T_l of the $Gd_{50}Co_{45}Al_5$ amorphous alloy are about 925 K and 939 K, respectively. Thus the reduced glass transition temperature T_{rg} ($=T_g/T_l$),[19] the parameter γ ($=T_x/(T_g+T_l)$), the critical cooling rate R_c ($=5.1\times10^{21}\exp(-117.19\gamma)$) and the critical section thickness Z_c ($=2.8\times10^{-7}\exp(41.7\gamma)$)[20,21] of $Gd_{50}Co_{45}Al_5$ are about 0.583, 0.396, 36 K/s and 4.16 mm, respectively. All of them are better than those of the $Gd_{50}Co_{50}$ amorphous alloy (T_{rg}=0.405, γ = 0.316, R_c=4.21×10^5 K/s, Z_c = 0.15 mm).[22] Therefore, the GFA of the $Gd_{50}Co_{50}$ amorphous alloy was obviously enhanced by Al addition.

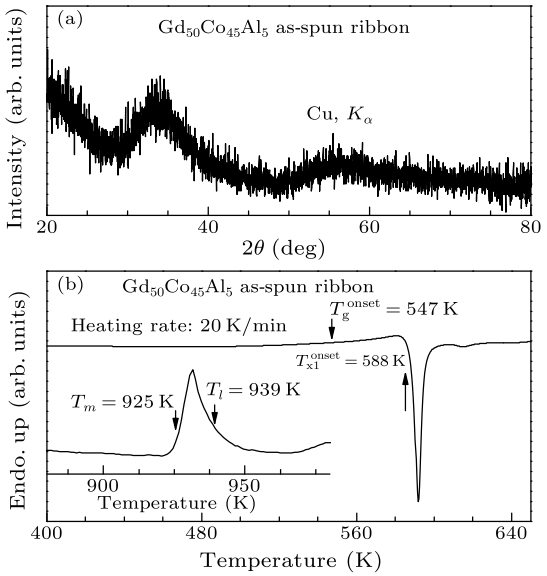

Fig. 1. (a) XRD pattern of the $Gd_{50}Co_{45}Al_5$ as-spun ribbon, (b) DSC trances of the $Gd_{50}Co_{45}Al_5$ as-spun ribbon. The inset is the melting behavior of the ribbon.

The mechanism of the improved GFA by Al addition can be explained from two points. From the structural point of view,[17,18] Al addition in the Gd–Co system leads to the atomic size mismatches among all constituents. According to the thermodynamic view,[23,24] the Al addition makes the formation enthalpy of amorphous (ΔH^{amor}) for the $Gd_{50}Co_{50}$-based alloy decrease from −40.2 kJ/mol to −43 kJ/mol. It makes the $Gd_{50}Co_{45}Al_5$ alloy take advantages to the formation of amorphous structure. The analysis indicates that the Al addition is beneficial for improving the glass-forming ability.

The M–T curves of the $Gd_{50}Co_{50-x}Al_x$ (x = 0, 5) ribbons were measured under the field of 0.03 T during the cooling process, as shown in Fig. 2. The Curie temperature of the $Gd_{50}Co_{50-x}Al_x$ (x = 0, 5) amorphous alloys have been determined to be the temperature at which the absolute value of dM/dT has a peak, as shown in the inset of Fig. 2. The values of T_C of the $Gd_{50}Co_{50}$ and $Gd_{50}Co_{45}Al_5$ ribbons are 267.5 K and 197.5 K, respectively. The value of T_C decreases with the Al addition as a replacement of Co.

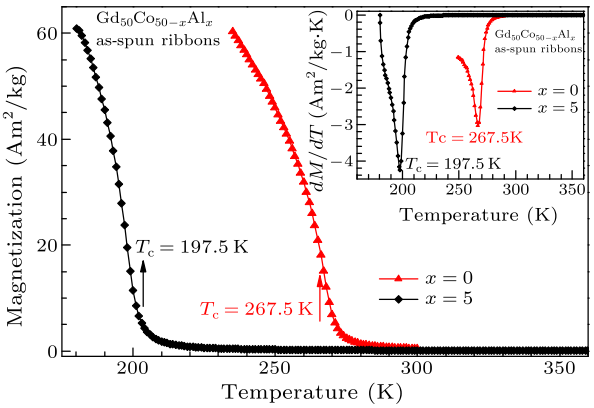

Fig. 2. The M–T curves of the $Gd_{50}Co_{50-x}Al_x$ (x = 0, 5) amorphous ribbons. The inset is dM/dT versus T.

In the $Gd_{50}Co_{50}$ binary amorphous alloy, there are three styles of exchange interactions: Gd–Gd, Gd–Co and Co–Co. The prevailing view is that the Co–Co interaction plays the most important role in determining the magnitude of the Curie temperature.[25,26] However, the Co–Co interactions can be influenced by the nearest atomic distance and the local environment of cobalt. As compared with the most rare earth (R)-transition metal (M) permanent magnet alloys, such as the Sm_2Co_{17} and the Gd_2Co_{17} alloys, the Co content in the $Gd_{50}Co_{50}$ alloy is significantly decreased. The Co–Co interactions are weakened by the increase of the nearest atomic distance of Co. At the same time, the interactions involving Gd (Gd–Gd and Gd–Co) play a more important role in determining the magnetic behavior. The carriers of magnetism in Gd are the 4f electrons, which locate deeply inside the atom. When the Gd atoms condense to form metals, the 5d electrons in the outer shells will be shared by many other atoms and contribute to electrical conductivity and metallic bonding. Moreover, these 5d electrons serve as a medium of exchange interaction, producing ordered arrangements of the 4f spins. In substance, the Gd–Gd and Gd–Co interactions are 4f–5d–4f and 3d–5d–4f indirect interactions, respectively.[25] The Curie temperature decreasing can be divided into three reasons: firstly, the Gd–Co interactions have weakened the Co–Co interactions. Secondly, the nearest magnetic atomic distance and the local environment of the magnetic atom are changed by the Al addition. Thirdly, the Al itself serves as an electron reservoir which provides s, p electron for Co 3d state filling and reduces the exchange behavior between 3d electrons, which further reduces the Co–Co interactions.[26]

The isothermal magnetic entropy change (ΔS_m) of the $Gd_{50}Co_{50-x}Al_x$ amorphous alloys are derived by using the Maxwell equation from M–H curves under

the field of 5 T,

$$\Delta S_{\rm m}(T,H) = S_{\rm m}(T,H) - S_{\rm m}(T,0) = \int_0^H \left(\frac{\partial M}{\partial T}\right)_H dH.$$

Figure 3 shows the $(-\Delta S_{\rm m})$–T curves of the $Gd_{50}Co_{50}$ and $Gd_{50}Co_{45}Al_5$ amorphous alloys under an applied field of 5 T for comparison. The broadened $-\Delta S_{\rm m}$ peak of the amorphous alloys reveals that the typical characteristics of the magnets undergo a second order magnetic phase transition. The broad peaks are caused by fluctuation of the exchange integral, resulting from the structural disorder of the material. The $-\Delta S_{\rm m}^{\rm peak}$ of the $Gd_{50}Co_{45}Al_5$ ribbon under 5 T is about 6.64 J·kg^{-1}K^{-1} at $T_{\rm C}$ (197.5 K), which is nearly 44% higher than that of the $Gd_{50}Co_{50}$ ribbon (about 4.6 J·kg^{-1}K^{-1} at $T_{\rm C}$ (267.5 K))[22] under the same magnetic field. In addition to $-\Delta S_{\rm m}^{\rm peak}$, there is another important parameter RC ($RC = -\Delta S_{\rm m}^{\rm peak} \times \Delta T_{\rm m}$, where $\Delta T_{\rm m}$ is the temperature range at the half maximum of $-\Delta S_{\rm m}^{\rm peak}$) evaluating the MCE of the magnets.[27] For the $Gd_{50}Co_{45}Al_5$ amorphous alloy, RC is about 764 J·kg^{-1} under 5 T, which is much larger than that of the $Gd_{50}Co_{50}$ alloy (about 686 J·kg^{-1} under 5 T)[22] and numerous magnetic materials previously reported.[12,28–31] The number of free electrons was increased with the Al addition. The free electrons also serving as a medium of exchange interaction will enhance $4f$–$4f$ and $3d$–$4f$ interactions, and contributed to the excess $-\Delta S_{\rm m}^{\rm peak}$ and RC.[32–34] The values of $-\Delta S_{\rm m}^{\rm peak}$ and RC under different magnetic fields of $Gd_{50}Co_{45}Al_5$ and other amorphous alloys are listed in Table 1.

Table 1. The values of $-\Delta S_{\rm m}^{\rm peak}$ and RC under different magnetic fields of $Gd_{50}Co_{45}Al_5$ and other amorphous alloys.

MCE of amorphous alloys		1 T	2 T	3 T	4 T	5 T	Reference
$Gd_{50}Co_{45}Al_5$	$-\Delta S_{\rm m}^{\rm peak}$ (J·kg^{-1}K^{-1})	2.04	3.42	4.6	5.66	6.64	Present work
	RC (J·kg^{-1})	111.2	256.9	408.5	579.8	764	
$Gd_{50}Co_{50}$	$-\Delta S_{\rm m}^{\rm peak}$ (J·kg^{-1}K^{-1})	1.38	2.36	3.16	3.92	4.6	Ref. [22]
	RC (J·kg^{-1})	89.6	212.8	366.9	507	686	
$Gd_{55}Co_{35}Ni_{10}$	$-\Delta S_{\rm m}^{\rm peak}$ (J·kg^{-1}K^{-1})					6.47	Ref. [12]
	RC (J·kg^{-1})					502	
$Gd_{55}Co_{30}Ni_{15}$	$-\Delta S_{\rm m}^{\rm peak}$ (J·kg^{-1}K^{-1})					6.30	Ref. [12]
	RC (J·kg^{-1})					487	
$Fe_{88}Zr_8B_4$	$-\Delta S_{\rm m}^{\rm peak}$ (J·kg^{-1}K^{-1})		1.3			2.8	Ref. [28]
	RC (J·kg^{-1})		201			551	
$Fe_{87}Zr_6B_6Cu_1$	$-\Delta S_{\rm m}^{\rm peak}$ (J·kg^{-1}K^{-1})		1.6			3	Ref. [28]
	RC (J·kg^{-1})		208			590	
$Gd_{60}Al_{10}Mn_{30}$	$-\Delta S_{\rm m}^{\rm peak}$ (J·kg^{-1}K^{-1})		1.4			3.3	Ref. [29]
	RC (J·kg^{-1})		210			660	
$Er_{65}Co_{35}$	$-\Delta S_{\rm m}^{\rm peak}$ (J·kg^{-1}K^{-1})					5.97	Ref. [30]
	RC (J·kg^{-1})					131	
$Fe_{78}Co_5Zr_6B_{10}Cu_1$	$-\Delta S_{\rm m}^{\rm peak}$ (J·kg^{-1}K^{-1})		1.6 under 1.5 T				Ref. [31]
	RC (J·kg^{-1})		82 under 1.5 T				

The normalized parameters, including the relative magnetic entropy change $(-\Delta S_{\rm m}/H)$ and the relative cooling power (RC/H),[29,35] are usually applied to evaluate the MCE of different materials due to the fact that $-\Delta S_{\rm m}^{\rm peak}$ and RC of the magnetic materials are usually obtained under different magnetic fields in literature. According to the $(-\Delta S_{\rm m})$–T curves of the $Gd_{50}Co_{45}Al_5$ amorphous alloy under different magnetic fields, as shown in Fig. 4, the normalized parameters change with the applied field obviously. For example, RC/H for the amorphous alloy is about 111.2 J·kg^{-1}T^{-1} under 1 T, 128.5 J·kg^{-1}T^{-1} under 2 T, 136.2 J·kg^{-1}T^{-1} under 3 T, 145 J·kg^{-1}T^{-1} under 4 T and 152.8 J·kg^{-1}T^{-1} under 5 T, respectively. Obviously, the normalized parameter is not a constant with the variation of applied field, indicating that the normalized parameters are no longer the valid way for evaluating the MCE obtained under different fields of magnetic materials.

To compare the magnetic properties of different materials under different test conditions, the $-\Delta S_{\rm m} \propto H^n$ was made to explain the field dependence of $-\Delta S_{\rm m}^{\rm peak}$ for the materials with a second-order phase transition. The n value does change with the temperature, $n = 1$ for the temperature well below $T_{\rm C}$; $n = 2$ for the temperature well above $T_{\rm C}$; $n \approx 0.72$ according to the Arnott–Noakes equation for the temperature near $T_{\rm C}$.[36] The $-\Delta S_{\rm m}^{\rm peak}$ versus H of the $Gd_{50}Co_{45}Al_5$ amorphous alloy was then plotted, as shown in the inset of Fig. 4, and the field dependence of $-\Delta S_{\rm m}^{\rm peak}$ follows a $-\Delta S_{\rm m}^{\rm peak} \propto H^n$ relationship. The calculated value of n ($n_{\rm cal}$) value of the $Gd_{50}Co_{45}Al_5$ ribbon is 0.736, which is close to the value near $T_{\rm C}$ of the master curve proposed by Franco *et al.*[36] The difference between n and $n_{\rm cal}$ is considered to be due to the microstructure of the amorphous alloys being much more complicated than that of a single phase alloy due to the presence of short-

range order (SRO), medium-range order (MRO) or even nano-crystallized (NC) structures embedded in the disordered matrix.

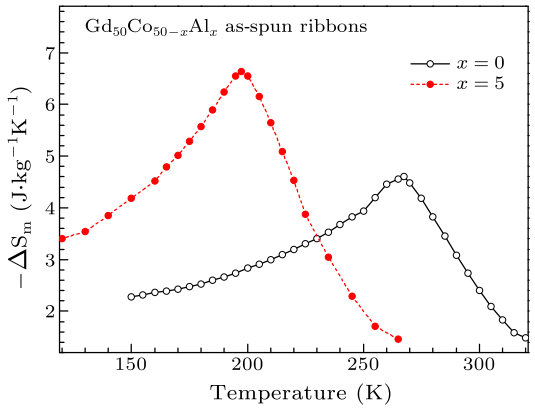

Fig. 3. The $(-\Delta S_{\rm m})$–T curves of the $Gd_{50}Co_{50-x}Al_5$ ($x = 0$, 5) amorphous ribbons under the applied field of 5 T.

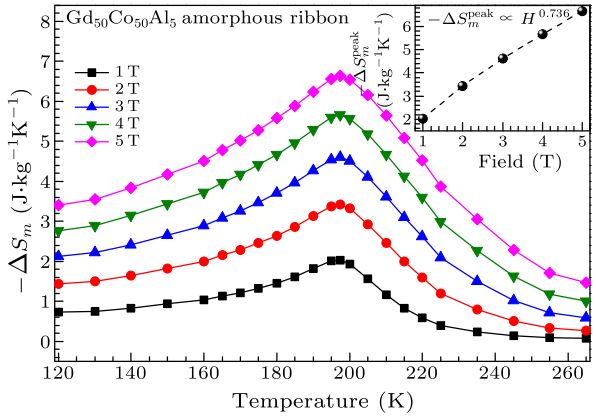

Fig. 4. The $(-\Delta S_{\rm m})$–T curve of the $Gd_{50}Co_{45}Al_5$ as-spun ribbon under the fields of 1 T, 2 T, 3 T, 4 T and 5 T. The inset is the field dependence of $-\Delta S_{\rm m}^{\rm peak}$ for the $Gd_{50}Co_{45}Al_5$ amorphous ribbon.

In summary, by Al substitution for Co on the $Gd_{50}Co_{50}$ amorphous alloy, we have obtained $Gd_{50}Co_{45}Al_5$ amorphous alloy with enhanced MCE. Magnetic measurements reveal that $T_{\rm C}$ (about 197.5 K under 0.03 T) is reduced by alloying addition. It is supposed to be due to the Al itself serving as an electron reservoir which provides s, p electrons for Co $3d$ state filling and reduces the exchange behavior between $3d$ electrons. Meanwhile, it reduces the Gd–Co and Co–Co interactions, which leads to $T_{\rm C}$ reducing. The values of $-\Delta S_{\rm m}^{\rm peak}$ (6.64 J·kg^{-1}K^{-1} at 197.5 K) and RC (about 764 J·kg^{-1}) of the $Gd_{50}Co_{45}Al_5$ amorphous alloy are higher than those of $Gd_{50}Co_{50}$ amorphous alloy indicating the enhanced MCE by Al addition. The field dependence of $-\Delta S_{\rm m}^{\rm peak}$ roughly follows the $-\Delta S_{\rm m}^{\rm peak} \propto H^{0.736}$ relationship near $T_{\rm C}$, which is similar to the situation of other amorphous alloys. The difference between n and $n_{\rm cal}$ is supposed to be induced by the obstructed magnetization of the amorphous alloys under low magnetic field due to the presence of the SRO, MRO, or NC structures.

References

[1] Gschneidner K A and Pecharsky Jr V K 2000 *Annu. Rev. Mater. Sci.* **30** 387
[2] Bruck E 2005 *J. Phys.* D **38** R381
[3] Inoue A 2000 *Acta Mater.* **48** 279
[4] Johnson W L 2002 *J. Minerals* **54** 40
[5] Wang W H, Dong C and Shek C H 2004 *Mater. Sci. Eng.* R **44** 45
[6] Inoue A 2011 *Acta Mater.* **59** 2243
[7] Du J, Zheng Q, Li Y B, Zhang Q, Li D and Zhang Z D 2008 *J. Appl. Phys.* **103** 023918
[8] Dong Q Y, Shen B Q, Chen J, Shen J, Wang F, Zhang H W and Sun J R 2009 *J. Appl. Phys.* **105** 053908
[9] Luo Q and Wang W H 2010 *J. Alloys Compd.* **495** 209
[10] Wang P, Chan K C, Lu S, Tang M B and Xia L 2012 *Chin. Phys. Lett.* **29** 096103
[11] Zhong X C, Tang P F, Liu Z W, Zeng D C, Zheng Z G, Yu H Y, Qiu W Q and Zou M 2011 *J. Alloys Compd.* **509** 6889
[12] Zhong X C, Tang P F, Liu Z W, Zeng D C, Zheng Z G, Yu H Y, Qiu W Q, Zhang H and Ramanujan R V 2012 *J. Appl. Phys.* **111** 07A919
[13] Yuan F, Du J and Shen B 2012 *Appl. Phys. Lett.* **101** 032405
[14] Ding D, Wang P, Guan Q, Tang M B and Xia L 2013 *Chin. Phys. Lett.* **30** 096104
[15] Xia L, Chan K C, Tang M B and Dong Y D 2014 *J. Appl. Phys.* **115** 223904
[16] Wu C, Yu P and Xia L 2015 *J. Non-Cryst. Solids* **422** 23
[17] Lu Z P and Liu C T 2004 *J. Mater. Sci.* **39** 3965
[18] Wang W H 2007 *Prog. Mater. Sci.* **52** 540
[19] Turnbull D 1969 *Contemp. Phys.* **10** 473
[20] Lu Z P and Liu C T 2003 *Phys. Rev. Lett.* **91** 115505
[21] Lu Z P and Liu C T 2002 *Acta Mater.* **50** 3501
[22] Xia L, Wu C, Chen S H and Chan K C 2015 *AIP Adv.* **5** 097122
[23] Boer F R De, Boom R, Mattens W C M, Miedema A R and Niessen A K 1988 *Cohesion in Metals, Transition Metals Alloys* (Amsterdam: North-Holland)
[24] Brkker H 1998 *Enthalpies in Alloys: Miedema's Semi-Empirical Model* (Switzerland: Trans Tech Publications)
[25] Belorizky E, Fremy M A, Gavigan J P, Givord D and Li H S 1987 *J. Appl. Phys.* **61** 3971
[26] Zhang J H, Liu S, Gu F, Yang L J and Liu M 2006 *Acta Phys. Sin.* **55** 2928 (in Chinese)
[27] Gschneidner K A Jr, Pecharsky V K and Tsokol A O 2005 *Rep. Prog. Phys.* **68** 1479
[28] Alvarez-Alonso P, Sánchez Llamazares J L, Sánchez-Valdés C F, Fdez-Gubieda M L, Gorria P and Blanco J A 2015 *J. Appl. Phys.* **117** 17A710
[29] Gorsse S, Chevalier B and Orveillon G 2008 *Appl. Phys. Lett.* **92** 122501
[30] Boutahar A, Lassri H, Zehani K, Bessais L and Hlil E K 2014 *J. Magn. Magn. Mater.* **369** 92
[31] Franco V, Blázquez J S and Conde A 2006 *J. Appl. Phys.* **100** 064307
[32] Chikazumi S and Graham Jr C D 1997 *Physics of Ferromagnetism* (Oxford: Clarendon)
[33] Pont M, Puig T, Rao K V and Inoue A 1992 *J. Appl. Phys.* **71** 4991
[34] Richter M 1998 *J. Phys. D: Appl. Phys.* **31** 1017
[35] Oesterreicher H and Parker F T 1984 *J. Appl. Phys.* **55** 4334
[36] Franco V, Blázquez J S and Conde A 2006 *Appl. Phys. Lett.* **89** 222512